

Accounts

Sol–Gel Process of Oxides Accompanied by Phase Separation

Kazuki Nakanishi

Department of Chemistry, Graduate School of Science, Kyoto University, Kitashirakawa, Sakyo-ku, Kyoto 606-8502

Received June 27, 2005; E-mail: Kazuki@kuchem.kyoto-u.ac.jp

A versatile sol–gel method for fabricating porous oxide materials with well-defined co-continuous macropores has been reviewed. The chemical instability, in many cases induced by polymerization of the network-forming components, triggers the formation of biphasic morphologies, followed by an irreversible freezing of the transient morphology by the sol–gel transition of the gelling phase. Upon removal of the non-gelling phase, an oxide framework comprising of controlled macropores can be obtained. The mesopore system of such macroporous materials can be further modified either by a physico-chemical treatment or a supramolecular templating technique. Pure silica and siloxane-based organic–inorganic hybrids with a hierarchical pore system in monolithic form have been successfully applied to the novel type of separation medium for high performance liquid chromatography, HPLC. Additional topics are also described including recent advances in the 3D-analysis of the interfacial properties of macroporous systems, extended compositional variations in the network-forming phase, and emerging applications in areas of biochemistry.

In the preparation of amorphous materials, the unstable or metastable state plays an important role in forming multi-phasic structures in the length scale longer than several nanometers. While in metastable states one often observes a formation of dispersed phases associated with thermally activated diffusion, unstable states are the starting points of various spontaneous morphology formation processes represented by the spinodal decomposition. In melt-quenching fabrication processes of oxide glasses, a pseudo one-phase material is initially formed by rapidly cooling a multi-component melt, and partially crystallized or phase-separated microstructures are controlled by subsequent reheating processes. The metastable glassy state is conveniently used to bring a system into a thermodynamically unstable region as well as to physically freeze the transient heterogeneous state at will. In a chemically polymerizing system, however, the polymerization and crosslinking reactions take place in the presence of a solvent. It is virtually impossible to physically freeze the reaction without influencing all the chemical interactions among the constituents. A continuous polymerization process is chemically equivalent to the continuous physical cooling with respect to the chemical interaction (mutual solubility) and material transport (mobility of the solutes). That is, the polymerizing system resulting in a sol–gel transition is a chemical analogue to a continuously cooled system resulting in a glass transition. If a process of developing heterogeneity in the system superposes a structure-freezing process, a competition will take place between the two processes. Various kinds of transient heterogeneous structures will be frozen in the resultant solidified materials.

Phase-separation phenomena related to the heterogeneity formation in materials have been investigated first in metallic alloys and oxide glasses, followed extensively by studies of polymeric materials mainly due to their slow dynamics of developing heterogeneity. In biphasic materials with co-continuous (or bicontinuous) domains, removal of either of the phases by selective extraction results in porous materials. An industrial process of fabricating well-defined porous silica-rich glasses has been established by Corning Glass Works about a half century ago.[1] Because the process included dissolution of alkali-borate glass phase out of the pre-formed phase-separated glass, it required a relatively long processing time depending on the thickness of the product. A chemically polymerizing system, on the other hand, often phase separates into network and solvent phases. Since the removal of solvent phase can be carried out more efficiently by evaporation, chemically-polymerized phase-separated structure can be a favorable basis for precisely controlled porous materials. In the present review, a polymerization-induced phase separation accompanied by a sol–gel transition is described, taking polysiloxane systems as major examples.

1. Formation of Macroporous Morphology by Phase Separation and Concurrent Sol–Gel Transition

1.1 Polymerization-Induced Phase Separation. In most so-called "sol–gel processing" of various metal oxides, metal alkoxides are popular starting materials. The hydrolysis and polycondensation behaviors of silicon alkoxides have been extensively studied because of the exceptionally slow reaction kinetics and, therefore, the ease of obtaining homogeneous-looking gels under ambient conditions. Oxide gels can be prepared also from colloidal particles dispersed in an appropriate fluid medium (usually an aqueous medium) by destabilizing

Published on the web May 12, 2006; DOI: 10.1246/bcsj.79.673

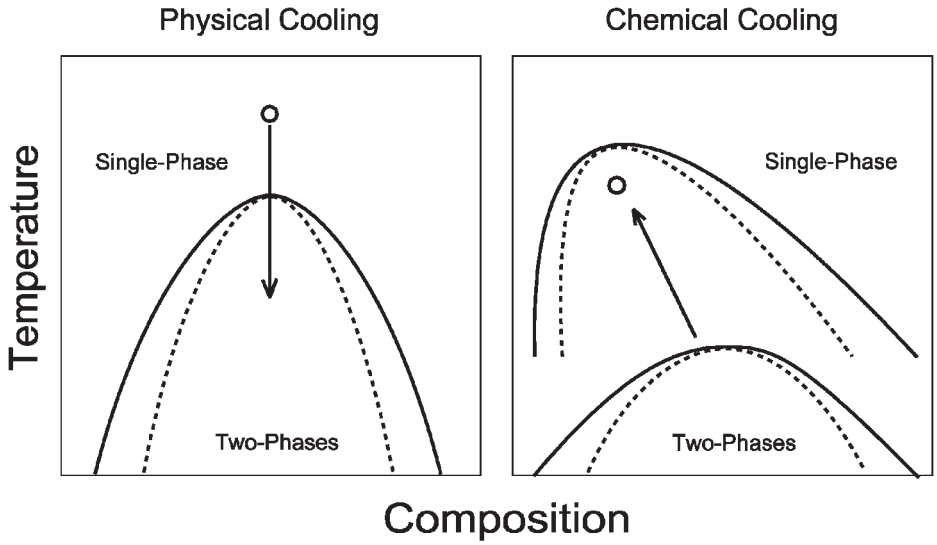

Fig. 1. Physical vs chemical cooling.

the dispersion. In the following theoretical part of the polymerization-induced phase separation, we in principle limit ourselves to chemical polymerization reactions, represented by polycondensation reactions of hydrolyzed metal alkoxides.

Let us first consider a typical hydrolysis–polycondensation of alkoxysilanes under acidic conditions, which gives a relatively narrow distribution of the molecular weight of the polymerizing oligomers.[2] The average molecular weight of the polymerizing species in a solution increases with reaction time by virtually irreversible polycondensation reactions among the monomers/oligomers. The thermodynamics of a solution containing polymerizing species tells us that mutual solubility among the constituents becomes lower as the average molecular weight of the polymerizing species increases.[3] This is mainly due to the loss of entropy of mixing among the constituents, which leads to the increase of the free energy of mixing, ΔG.

$$\Delta G = \Delta H - T\Delta S. \quad (1)$$

The reduction in mutual solubility caused by polymerization can be contrasted with that caused by physical cooling of the system[4] (See Fig. 1). In the latter case, the free energy of mixing is increased by lowering temperature. In both cases, a multicomponent system becomes less stable as the absolute value of the $T\Delta S$ term decreases. In some cases, changes in the polarity of oligomers with the generation and/or consumption of silanol groups may contribute to increase the ΔH term, which will also destabilize the system against homogeneous mixing. In any case, when the sign of free energy of mixing of the system becomes positive, the thermodynamic driving force for phase separation is generated.

In real experimental systems, poor solvents of the oligomers, several kinds of water-soluble polymers, and cationic or nonionic surfactants can be used as an additive component to induce the phase separation in the course of a sol–gel reaction. Typical examples follow.

1.1.1 Low-Water Hydrolysis of Tetraalkoxysilane or Trialkoxy(alkyl)siloxane: When hydrolyzed with an understoichiometric amount of water ($H_2O/Si < 2$ and 1.5 in the cases of tetraalkoxysilane and trialkoxy(alkyl)siloxane, respectively), the siloxane oligomers retain a considerable amount of unreacted alkoxy groups. This condition is specified as "low-water" while the hydrolysis conducted under the presence of abundant water relative to that corresponding to the stoichiometric ($H_2O/Si = 2$) will be denoted as "high-water" in the following classifications. These oligomers with relatively low polarity tend to phase separate against a highly polar solvent mixture. Addition of an extremely high concentration of a mineral acid or formamide is preferable to induce phase separation in the solution derived from tetraalkoxysilanes.[5] With trialkoxy(alkyl)siloxanes, the generated oligomers have inherent hydrophobic groups and thus exhibit higher phase-separation tendency even against the mixtures of water and alcohol with a dilute acid catalyst.

A series of exceptions has been found recently with bridged alkoxysilanes. Bis(trialkoxysilyl)alkanes with C_6 or C_8 bridging alkylene chains typically phase separate against 50–70 fold molar amount of water relative to silicon under acidic conditions.[6] Relatively long alkylene chains buried in the siloxane network only moderately contribute to enhance the phase-separation tendency of the polymerizing oligomers.

1.1.2 High-Water Hydrolysis of Tetraalkoxysilane in the Presence of Weakly-Interacting Additives: With a sufficient amount of water, almost all the alkoxy groups are hydrolyzed into silanol groups. The polarity of the resultant siloxane oligomers is high enough to be dissolved in alcohol–water solvent mixtures containing ionic catalysts. An addition of a water-soluble polymer such as poly(acrylic acid) or poly(sodium 4-styrenesulfonate) to this system can induce the phase separation, mainly based on the incompatibility between the polymer and siloxane oligomers.[7,8] The added polymer is preferentially distributed to the phase containing minor amounts of siloxane oligomers, thus constituting the "fluid phase" in contrast to the "gel phase" rich in siloxane oligomers. In this case, the additive component plays an assisting role to induce the phase separation to form micrometer-range heterogeneous structures.

1.1.3 High-Water Hydrolysis of Tetraalkoxysilane or Alkylene-Bridged Alkoxysilane in the Presence of Hydrogen-Bonding Additives: Several surfactants and water-solu-

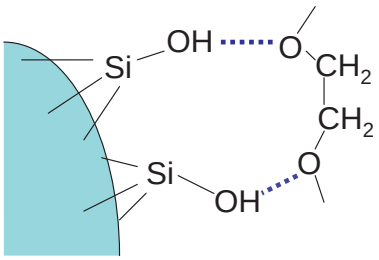

Fig. 2. Hydrogen bonding of PEO chains on surface silanols.

ble polymers are known to exhibit strong hydrogen-bonding interaction between silanol groups on the surfaces of silica colloids and in siloxane oligomers. Poly(oxyethylene) chains, for example, specifically form strong hydrogen bonds with silanols by their ether oxygens. When the poly(ethylene oxide), PEO, or surfactants containing poly(oxyethylene) units are added to the hydrolysis/polycondensation of alkoxysilanes, they form hydrogen-bonded amorphous complexes as soon as sufficient amounts of continuous silanol sites are generated as a result of polycondensation of hydrolyzed alkoxysilanes in the solution (Fig. 2). In the case that surfactants and polymers cover silanols so strongly that any further polycondensation is inhibited by the adsorbed molecules, only low molecular weight oligomers will segregate to form a dispersed, non-gelling phase. By an appropriate choice of the HLB value or the molecular weight, on the other hand, the phase separation can be concurrently induced with the homogeneous sol–gel transition of the reaction system.[9] Unlike the cases with weakly-interacting polymers, most of the additive surfactants or polymers are distributed to the phase to which majority of the siloxane oligomers are also distributed, and form a gel phase together. The fluid phase is then composed mainly of the solvent mixture.

The system containing hydrogen-bonding additives has an advantage in controlling the pore structure of the resultant gels. As will be explained in detail below, the sizes of the pores (to be more exact, the sizes of the separated phase domains) primarily depend on the phase-separation tendency of the polymerizing siloxane oligomer solution. The pore volume is determined mainly by the volume fraction of the fluid phase, and thus is roughly proportional to the concentrations of water and solvent in the starting composition. The pore size and the pore volume of a gelled material can be independently controlled by adjusting the concentrations of the additive and the solvent, respectively. In Section **1.1.2** described above, the phase-separation tendency and the volume fraction of the pore-forming phase are mutually interdependent, which makes it difficult to design a wide variety of pore structures.

1.2 Morphology Development by Spinodal Decomposition. In a phase diagram with a miscibility window, the two-phase region is divided into two sub-regions. One is that between binodal and spinodal, called the metastable region. In the metastable region, any infinitesimal fluctuation of the composition is energy-consuming, that is, finite activation energy is required to develop phase-separated domains. The typical phase-separation mechanism in this region is the "nucleation and growth" where dispersed small regions called nuclei grow accompanied by an addition of constituents diffusing

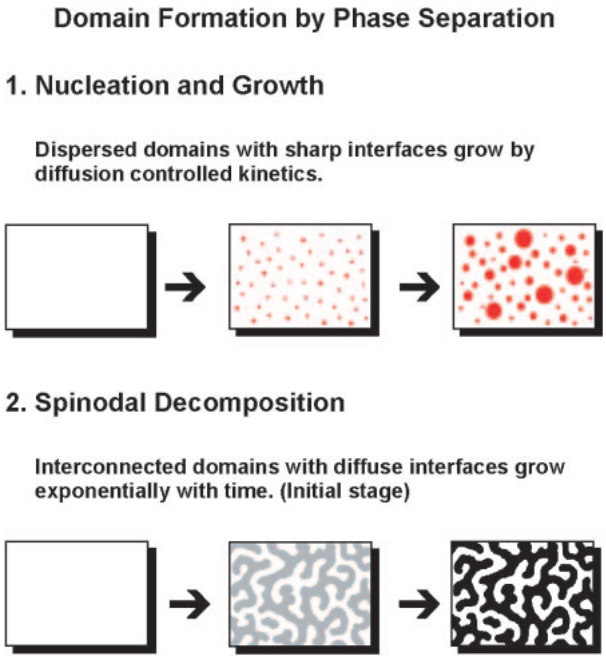

Fig. 3. Nucleation & growth and spinodal decomposition mechanisms.

from the bulk (not yet separated) regions of the system. The natural consequence of this mechanism is a morphology with "dispersed A" and "matrix B" phase domains (Fig. 3). The other region is that within a spinodal line, called the unstable region. In the unstable region, any infinitesimal fluctuation gains energy so that the fluctuation spontaneously develops with time without requiring any activation energy. Depending mainly on the depth of quench (the difference between the critical temperature and the actually quenched temperature) and the mobility of the constituents (more precisely, that of diffusing units), only a single Fourier component among the various fluctuation wavelengths survives and this component dominates the characteristic size of the domains. One clear difference that can be seen between the nucleation and growth mechanism is that the phase domains have no distinct interface in the initial stages of the phase separation. The contrast in chemical composition develops continuously with time until the equilibrium phase compositions are reached. Under comparable volume fractions of conjugate phase domains without crystallographic or mechanical anisotropy, a sponge-like structure called a co-continuous structure forms (Fig. 3). The co-continuous structure is characterized by mutually continuous conjugate domains and hyperbolic interfaces.

In the classical description of the initial stage of spinodal decomposition, the co-continuous structures are reproduced by the superposition of a number of sinusoidal compositional waves. The real structure development, however, strongly depends on the dynamics driven by the interfacial energy.[10] With an increase of concentration difference between the conjugate phase domains, the interfacial energy piles up. In order to reduce the total interfacial energy, the system reorganizes the domain structure toward that with less interfacial area and less local surface energy. The former can be achieved by coarsening the structure (Fig. 4). The self-similar coarsening of the

Fig. 4. Time evolution of spinodally decomposing isotropic symmetrical system.

spinodally phase-separated domains is well known in many oxide glass or organic polymer systems. Since the co-continuous structure of spinodal decomposition contains both negative and positive curvature surfaces, a curvature of either sign should be eliminated to attain the most stable interfacial configuration. The fragmentation of either of the conjugate phases is the result of the latter local surface-energetic requirement. As shown in the figure, the well-defined co-continuous structure of the spinodal decomposition is a transient structure, which coarsens self-similarly for a limited duration of time and then breaks up into fragmented structures.

1.3 Structure Freezing by Sol–Gel Transition. Sol–gel transition is a phenomenon which strongly depends on the network connectivity. In the case of virtually irreversible chemical sol–gel transition in a solution, a constant increase in the degree of polymerization of individual clusters contributes to increase the solution viscosity only gradually in the earlier stage of polymerization. The continued growth of clusters, however, reaches a point where the first single connection across the system dimension is formed. Around this point, typically denoted as the sol–gel transition point, the steep increase and divergence of viscosity is observed, and, in parallel, the system turns from a viscous fluid to an elastic solid. Due to the continued polymerization reactions within the loosely connected network, the network density gradually increases to arrest motions of constituents in increasingly finer dimensions.

If any transient (dynamic) heterogeneity is present in a gelling solution, it will be arrested in the gel network when the timescale of the sol–gel transition is short enough to freeze the "snap-shot" structure of the transient heterogeneity. In the sol–gel system based on an acid-catalyzed hydrolysis–polycondensation of alkoxysilane, both the structural evolution due to phase separation and the structure freezing by sol–gel transition take place as a result of irreversible polycondensation reactions. The "frozen" structure depends, therefore, on the onset of phase separation relative to the "freezing" point by sol–gel transition. The earlier the phase separation is initiated relative to the sol–gel transition, the coarser the resultant structure becomes, and vice versa.

Among numerous reaction parameters of a sol–gel reaction, those that strongly influence the mutual solubility of the constituents and/or the hydrolysis–polycondensation reaction rates play important roles in determining the final size of the phase-separated domains in the gels. For example, a higher reaction temperature normally increases the mutual solubility of the constituents and hence suppresses the phase-separation tendency, and in parallel it accelerates the hydrolysis–polycondensation reactions. Due to these duplicate effects, gels with drastically finer phase-separated domains are obtained at higher temperatures. If one adds a co-solvent of the relatively incompatible components in the reaction solution, the phase-separation tendency is suppressed usually accompanied by decreased hydrolysis–polycondensation reaction rates due to the dilution effect. In this case, the resultant morphology depends on the competitive effects of suppressed phase separations and decelerated hydrolysis–polycondensation reactions.

Another important parameter which determines the gel morphology is the relative volume fraction of the "fluid" phase which converts to macropores after drying. With an exception of Section **1.1.2**, the "fluid" phase is usually that mainly composed of the solvent mixture. The volume fraction of the solvent then becomes a crucial parameter in determining the pore volume and overall connectivity of the gel skeletons in the resultant gel structure. With an appropriate choice of these reaction parameters, the pore size (domain size) and pore volume of the gels can be designed in a wide variety of morphologies (See Fig. 5).

1.4 Effect of Spatial Confinement on Macroporous Morphology. The formation of discrete three-dimensional phase-separated domains is identical to the development of interfaces between the conjugate phase domains. That is, the local morphology of phase-separating system may be affected by the presence of additional interfaces, such as substrate surfaces or container walls.

By dip-coating the phase-separating reaction solution, the developing domains in the coated layer are rapidly solidified by an evaporation-induced gelation. Such rapid freezing of the transient structure results in various two-dimensionally phase-separated structures on a substrate. Due to the presence of free surfaces contacting the atmosphere, asymmetric structures in the depth direction are often observed, depending mainly on the affinity of the gel phase to the substrate. In the case that the gel phase tends to wet and spread on the substrate surface, the domains of solvent phase are expelled from the substrate. This results in relative pore segregation in the upper part of the coating. With a substrate which has moderate affinity to both the gel and the solvent phases, phase-separated domains with completely homogeneous structure in the thickness direction can be observed (Fig. 6).

In the absence of the physically-induced solidification process, such as cooling or evaporation of the solvent, the phase-separating domains are solidified by chemical crosslinking reactions that take place competitively with the phase-separation processes. In a two-dimensional (2D) confined space, e.g. a slab-shaped gap between parallel plates, the local deformation can be observed mainly in the vicinity of container walls.[11,12] We here limit our discussion to the morphology

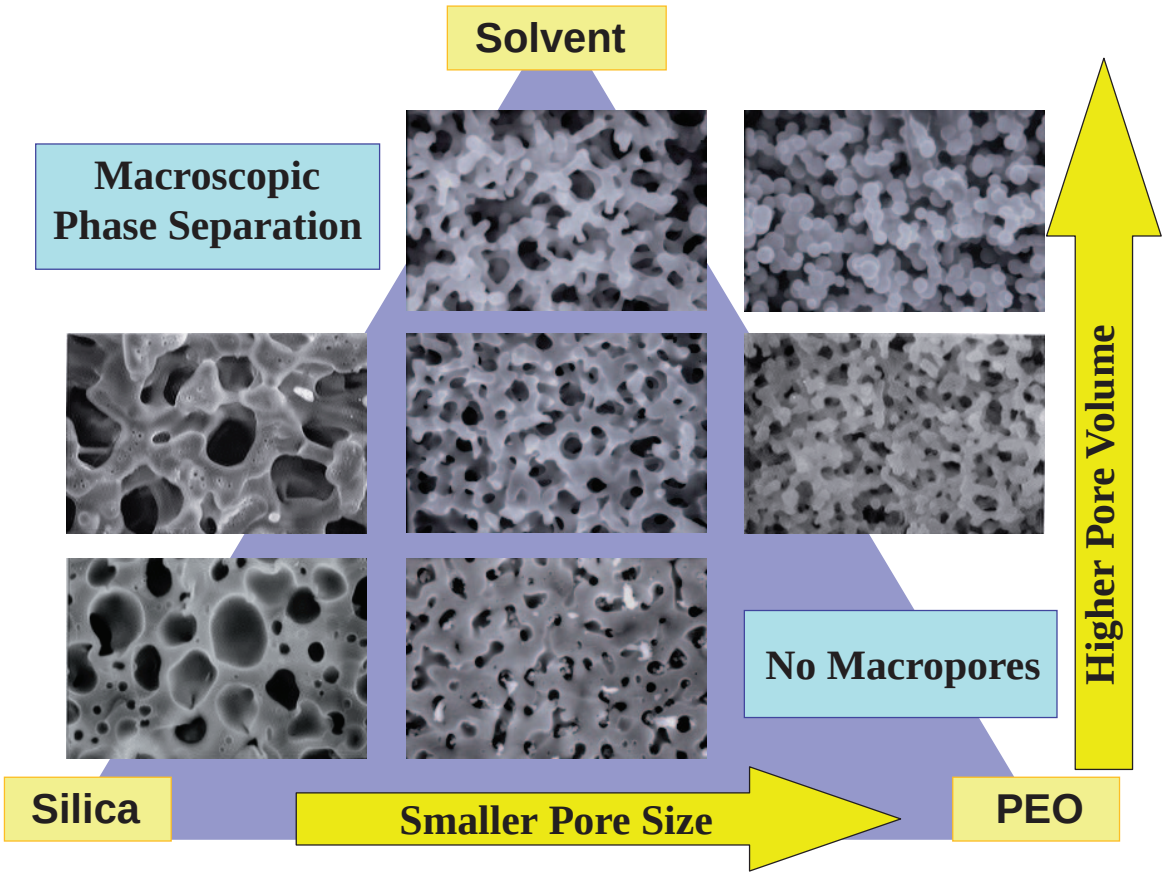

Fig. 5. Starting composition and resultant gel morphologies.

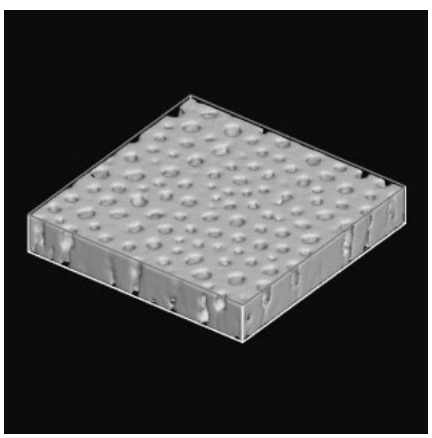

Fig. 6. Two-dimensional phase separation.

with co-continuous gel- and solvent-phases. Wetting and spreading of the gel phase onto the container walls in the course of domain formation (especially coarsening) results in the depletion layers just below the walls. The local pore volume of the wall-regions becomes significantly higher than that of the bulk-region which is not much influenced by the walls. In many cases, the phase-separated gel domains that originally have hyperbolic surfaces deform to columnar shapes normal to the wall surfaces (see Fig. 7). When the characteristic size of phase separation, denoted as Λ_m, typically the size of a set of conjugate domains, becomes larger than the dimension confined by the walls, the phase-separating gel domains transform from co-continuous skeletons to wetting layers on the walls (Fig. 7c). In the 2D confinement, detailed geometrical analysis on the interface structure has been carried out using laser scanning confocal microscopy (LSCM).[12]

In a one-dimensional (1D) confined space, experimentally a long enough capillary, the deformation and wetting becomes still more pronounced than in the case of 2D. In the cross-sectional view under SEM, the deformed domains often dominate the overall morphology (Fig. 8). A transition from co-continuous domains to a wetting layer is also observed.

Experiments on zero-dimensional (0D) confinement have also been performed using well-defined macroporous cages described above with the purpose of confirming the effect of limited material transfer. When the characteristic size of phase-separating domains becomes comparable to the confined dimension, extraordinary morphologies including extremely fine or significantly elongated domains can be observed. Homogeneous wetting on the inner surface of the macroporous host is possible, similarly to the cases of confinements in the higher dimensions.

1.5 Macropore Formation in Colloidal Sol–Gel Systems. Colloidal dispersion of oxide particles is one of the cost-effective precursors of porous materials compared with corresponding metal alkoxides. An efficient process to control macroporous structure in alkaline silicate—colloidal silica mixtures has been established by Shoup et al.[13] The gelation of alkaline silicate (so called water-glass) was modified by the colloidal

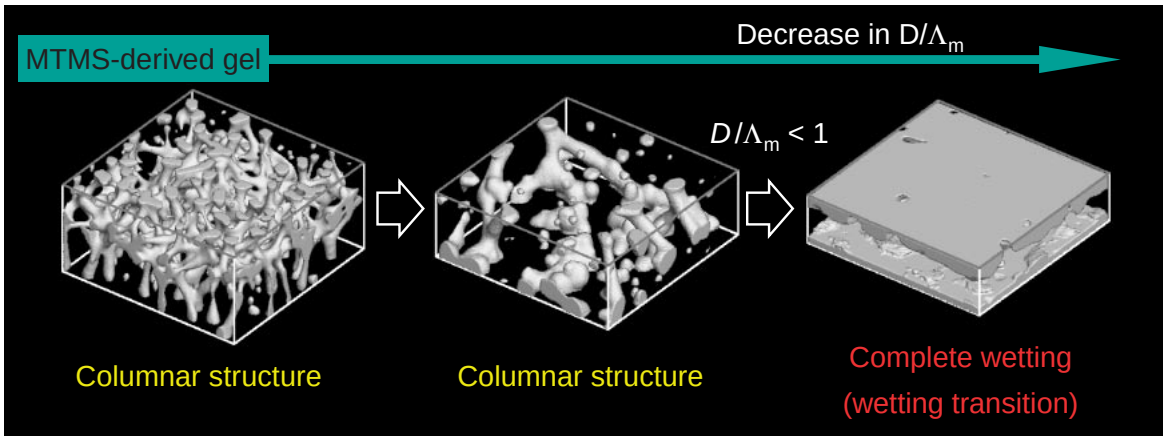

Fig. 7. Phase separation in 2D confined space.

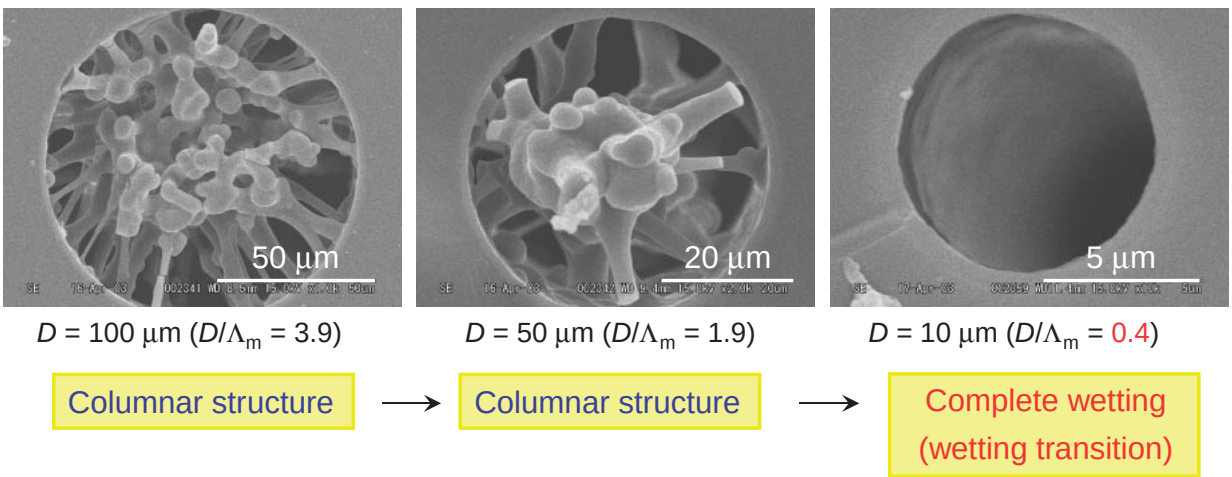

Fig. 8. Phase separation in 1D confined geometry.

particles to give continuous macropores up to sub-micrometers in diameter. Due to the inclusion of a considerable amount of rigid particles in a gel, as well as to the presence of continuous macropores which efficiently transport the solvent liquid, the drying shrinkage of the gel was effectively suppressed to avoid cracking and fracture. High silica glass products can be manufactured through the process by molding the gelling solution into various shapes.

Alkoxides of metals other than silicon generally exhibit much higher reactivity toward hydrolysis–polycondensation than those of silicon, mainly due to the difference in partial charge of the metals in their respective oxygen-coordinated environments. As a result, it is virtually impossible to control the gelation reaction with alkoxides of titanium or zirconium without significantly diluting the reaction system.[48] Although a vast range of applications with photocatalytic activity is expected, well-defined macroporous titania could not be synthesized in monolithic form. Here, we tried to solidify an aqueous dispersion of commercially available fine colloidal anatase while inducing the phase separation in the course of gelation (Table 1). By adding formamide to an acid-stabilized colloidal anatase dispersion at elevated temperature, we could increase the pH of the dispersion gradually and homogeneously. With an addition of poly(ethylene oxide), PEO, with relatively high molecular weight, typically higher than 100000, starting compositions were found which give well-defined macroporous morphology in resultant monolithic gels.[14] Results also revealed that added PEO preferentially distributed to the gel-phase and that the continuity of the gel skeletons improved with an increase of molecular weight of incorporated PEO. Selected SEM photographs and a representative pore size distribution curve are shown in Fig. 9. The appearance of the gel skeletons which constitute the continuous macroporous framework is very similar to those seen in alkoxide-derived gels. Although the mechanical strength of the colloidal wet gel is lower than that of alkoxide-derived gels, once dried carefully by freeze-drying, the macroporous monolithic samples can be heat-treated without fracture or deformation. The crystalline system transforms from anatase to rutile by heating up to ca. 900 °C. The colloidal route to macroporous oxide gels will be a versa-

Table 1. Starting Compositions of TiO_2 Colloid–PEO–Formamide–Nitric Acid System (Unit: g)

TiO_2	PEO (w_{PEO})	HNO_3	Formamide	Water
1.98	0.030–0.040	0.177	1.16	5.84

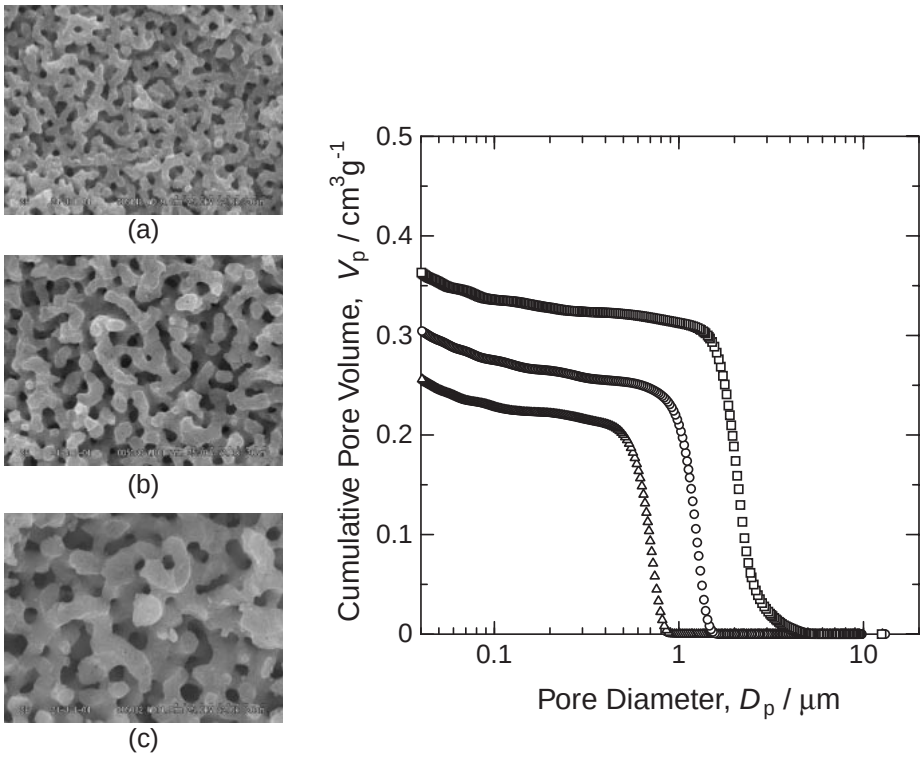

Fig. 9. SEM photographs of macroporous titania and pore size distribution. (a) $w_{PEO} = 0.030$; triangle, (b) $w_{PEO} = 0.035$; circle, (c) $w_{PEO} = 0.040$; square.

tile method since various kinds of useful oxide dispersions will be prepared into well-defined macroporous assemblages.

1.6 Prerequisite for Polymerization-Induced Phase Separation in Oxide Sol–Gel Systems. In the preceding section, the origins of polymerization-induced phase separation have been classified into entropy- and enthalpy-driven cases. We implicitly assumed that the classification is valid within the network-forming systems based on chemical polymerization. Among the enthalpy-driven cases, however, systems that incorporate strongly hydrogen-bonding additives behave similarly to each other irrespective of the kind of interaction, chemical polymerization or physical aggregation, which forms the gel network. The alkoxide-derived gels are composed of polymeric molecules connected with covalent bonds while the colloidal gels have physically aggregated particles as structural units. Considering the common features of these experimental systems, we assume that the following conditions and sequences are prerequisites for concurrent phase separation and sol–gel transition in oxide systems.

(a) A gel-forming component forms continuous M–OH sites on the surface of oligomers or aggregates either by polycondensation or by physical aggregation.

(b) Strongly hydrogen-bonding additives are adsorbed on the hydrophilic surface sites of the oligomers or aggregates. In the case that the additive is a hydrogen-bonding polymer, the strength of adsorption is often enhanced when an appropriate amount of continuous M–OH sites is available.

(c) The hydrogen-bonding additives break their solvated (hydrated) moieties to preferentially adsorb on the surfaces of oligomers or aggregates. Consequently, relatively hydrophobic parts of the additive molecules are exposed toward the surrounding solvent. Oligomers or aggregates thus adsorbed by the hydrogen-bonding additive exhibit decreased compatibility with the surrounding polar solvent mixtures, since they "wear" a molecular coverage with less polar surface sites. The hydrogen bonding of the additives, however, is not strong enough to completely prevent further polycondensation or aggregation among the oligomers or aggregates, which finally form infinitely crosslinked gel networks.

(d) The driving force of phase separation described above continues increasing parallel to the overall growth of oligomers or aggregates. Once the phase separation takes place, the dynamics of the gelling phase domains strongly adsorbed by the hydrogen-bonding additive is governed by a relatively viscous component. When the poly(ethyleneoxide), PEO, with substantially high molecular weight is incorporated in a gelling system, the dynamics of developing gel-phase depends mostly on the viscosity (or viscoelasticity) not of the oligomers or aggregates but of PEO.

The above mechanism explains the versatility of PEO (and possibly other hydrogen-bonding polymers) in both alkoxide and colloidal systems to control phase separation to give highly continuous gel domains. There are also systematic data of formation of macroporous gels in water-glass systems incorporated with water-soluble polymers.[15–18] In these cases, probably due to the inherent high viscosity of water-glass, the phase-separation dynamics is governed by both the gelling component and polymeric additives.

1.7 Advances in Macroporous Structural Characterization. The quantitative structural characterization of macroporous substances is usually performed by mercury porosimetry. By the successive incremental pressurization of liquid mercury

into an evacuated porous sample, the incremental intruded volume is measured as a function of applied pressure. This is converted to the pore size, d_p, via Washburn's equation.

$$d_p = -4\gamma \cos\theta / P, \tag{2}$$

where γ: the surface tension of mercury, θ: the contact angle between mercury and solid, and P: the intrusion pressure. Since mercury is intruded from the surface to the interior of the sample specimen, the geometry and connectivity of pores influence the measured pore size distribution. If larger pores are located behind narrow channels, the larger pores will not be accessed until the intrusion pressure is increased to a value that can intrude through the narrow channels. The "pore-blocking effect" thus becomes a major cause of errors in determining the pore size distribution by mercury porosimetry. Depending on the degree of blocking, the sizes of blocked pores are systematically underestimated.

As partly shown in the preceding sections, with an introduction of laser scanning confocal microscopy, LSCM, detailed information on the local geometry of heterogeneous systems has become available. Three-dimensional (3D) observation of porous silica monolith has first been performed by Jinnai et al. by chemically modifying the surface of a fully sintered silica skeleton with fluorescent dye.[19] Additional improvements were made to observe wet gels using appropriate contrast-matched solvents both in "positive" and "negative" modes where the fluorescent dye is impregnated into gel skeletons and macropores, respectively.[12,20] Figure 10 shows a schematic instrumentation setup of LSCM (LSM5 PASCAL, Carl Zeiss, Germany). A laser with 488 nm wavelength was used to excite a dye molecule (fluorescein). A long pass filter (LP505) was installed in front of photomultiplier in order to detect only the fluorescent light (approximately 519 nm).

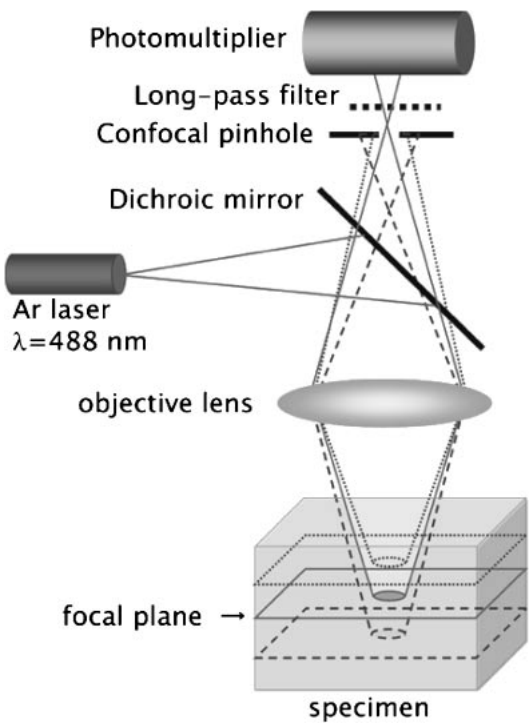

Fig. 10. Schematic setup of laser scanning confocal microscope, LSCM.

The laser was scanned in the lateral plane, measuring fluorescent intensity in a two-dimensional optically sliced image composed of N^2 ($N = 512$) pixel,[2] where N is the number of pixels along the edge of the two-dimensional image. Subsequently, the LSCM images were noise-filtered, digitized and finally reconstructed into 3D by stacking the digitized 2D images (Fig. 11). The porosity can be measured by counting the pixels designated to "pores" in the series of digitized images. The pore diameter is measured by drawing lines in 341 random directions in an obtained 3D image, counting the number of pixels for pore domain on every drawn lines and taking the most probable value for each length by Gaussian fitting (chord-length method).

For the purpose of further extracting quantitative geometrical information of macropore surface, we calculated the curvature on every point of the skeletons from the 3D images obtained by the above procedure. The curvature of the site of an arc is equal to the reciprocal of the radius of a circle that best fit to the curve at the site (an osculating circle). Similarly, local principal curvatures, κ_1 and κ_2, on a curved surface are defined as reciprocals of the radius of the largest and the smallest osculating circles, R_1 and R_2, respectively, at the same point (Fig. 12).

$$\kappa_i = \frac{1}{R_i}, \quad i = 1 \text{ or } 2. \tag{3}$$

Note that here a curvature is classified as positive if its osculating circle locates in the pore region, as negative if it locates in the skeleton region, and as equal to zero at the surface. The local mean curvature, H, and the Gaussian curvature, K, are defined as below using local principal curvatures.

$$H = \frac{\kappa_1 + \kappa_2}{2}, \quad K = \kappa_1 \cdot \kappa_2. \tag{4}$$

The obtained three-dimensional images from macropore surface observation by LSCM were subjected to an analysis of probability density distributions of the local curvatures by sectioning and fitting method (SFM). The numerical procedures and the precision of SFM are detailed elsewhere.[21]

Figure 13 shows typical model two-phase systems with simplified interface curvatures and corresponding probability density distributions. From local curvature distribution, we can estimate which kind of surface (i.e. parabolic, hyperbolic, or elliptic) is dominant on the measured overall macropore surface. Any realistic curvature set falls outside the $K = H^2$ boundary on which the curvature of elliptic surface is represented (except for the origin). As shown in the figure, the morphology of two-phase system inverts across the $H = 0$. According to the definition of the curvatures described above, local curvature values located in $H > 0$ and $K > 0$ are indicative of elongated or isolated pores, and those in $H < 0$ and $K > 0$ are indicative of elongated or fragmented gel skeletons. It has been demonstrated that the co-continuous two-phase structure typically developed by spinodal decomposition with 50:50 volume fractions without any dynamic asymmetry can be classified to the hyperbolic surface ($H = 0$ and $K < 0$).

The local curvature distributions of real macroporous monolithic silica are plotted in Fig. 14 as a function of porosity, ε. For the measured geometry data, the local curvature distribu-

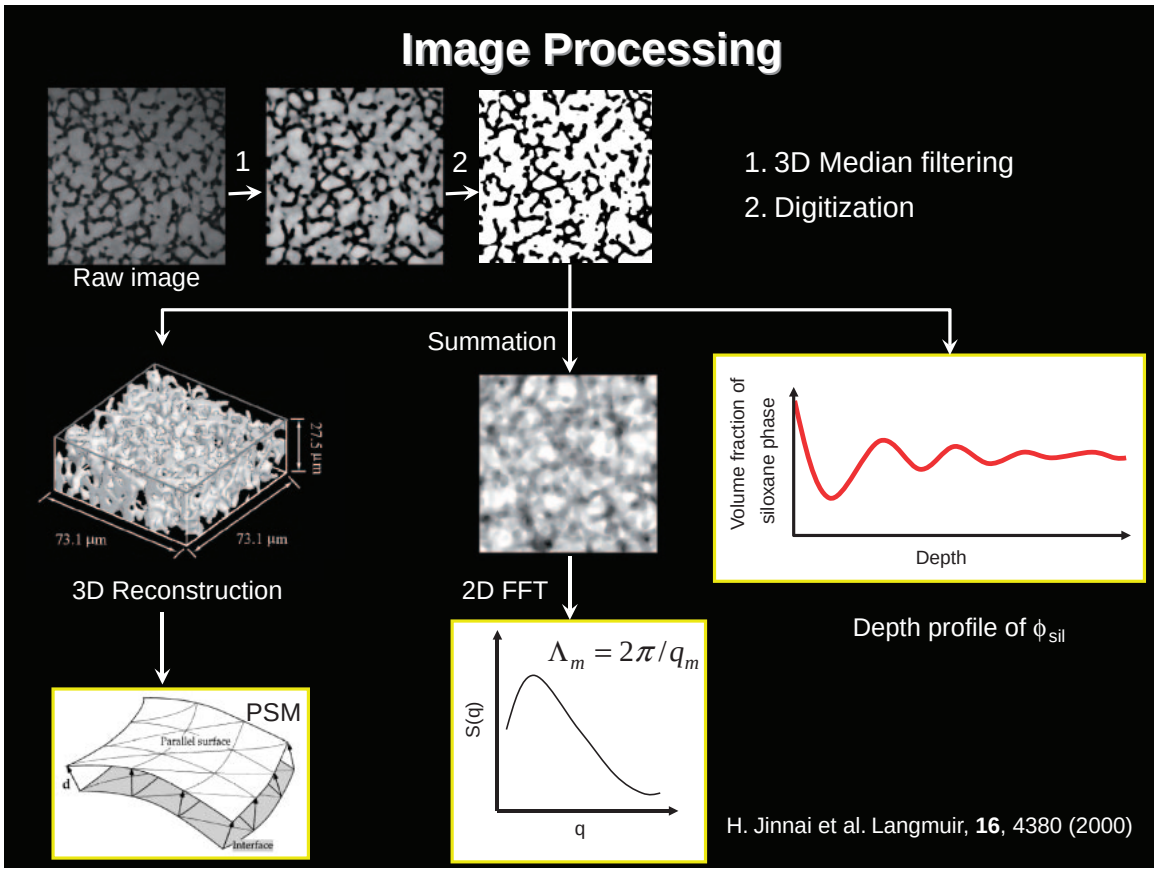

Fig. 11. Digital image processing of LSCM images.

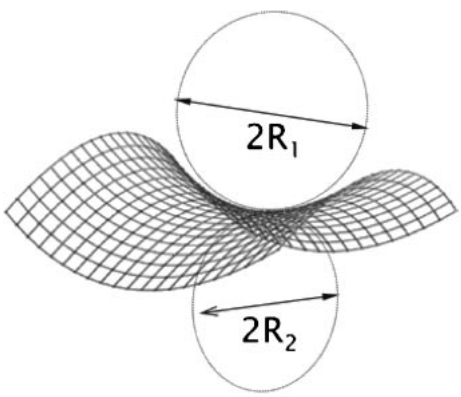

Fig. 12. Definition of principal curvatures on a curved surface.

tions calculated by SFM have been scaled with the inverse of the specific surface area, Σ^{-1} ($\Sigma = S/V$, S and V corresponds to total macropore surface area and total sample volume, respectively) to eliminate the influence of structure dimensions. The inverse of specific surface area is one of the characteristic length parameters of phase-separating structure and has been employed to scale geometrical parameters obtained from 3D images (i.e. local curvatures and area averaged curvatures).[19] At relatively low porosity, the distribution is asymmetrical, with an "arm" extended to the $H > 0$ and $K > 0$ region indicating the presence of elongated pores where the pore-blocking effect of the mercury intrusion method is pronounced. With an increase of porosity, the overall distribution becomes nearly symmetrical around $H = 0$ and $K < 0$, and further increase in porosity results in the elongation and fragmentation of the gel skeletons. At higher porosities, the pore-blocking effect is expected to become negligible. It was indeed proven that the median pore size measured by mercury intrusion method and that by LSCM image analysis agreed better with each other at higher porosities. Quantitative as well as statistical 3D real image analysis will become more important in investigating the macroporous structure prepared in small confined spaces, where direct and quantitative intrusion of mercury becomes impossible.

2. Tailoring Mesopores to Obtain Hierarchical Pore Structures

2.1 Post Gelation Aging of Silica Gels. Since the interconnected macropores enhances the material transport within the bulk gel sample, the exchange of pore liquid with an external solvent can be performed much faster than for the case with gels having only meso- to micropores. Conventional methods of tailoring mesopore structure by aging wet silica gels under basic and/or hydrothermal conditions can be suitably applied to the monolithic macroporous silica gels without essentially disturbing the well-defined macroporous structure. Experimentally, the as-gelled wet monolithic specimen is immersed in an excess amount of an external solvent such as aqueous ammonia solution. Alternatively, one can add urea in the starting composition of the gel preparation, and subsequently heat the wet gel in a closed vessel to generate aqueous

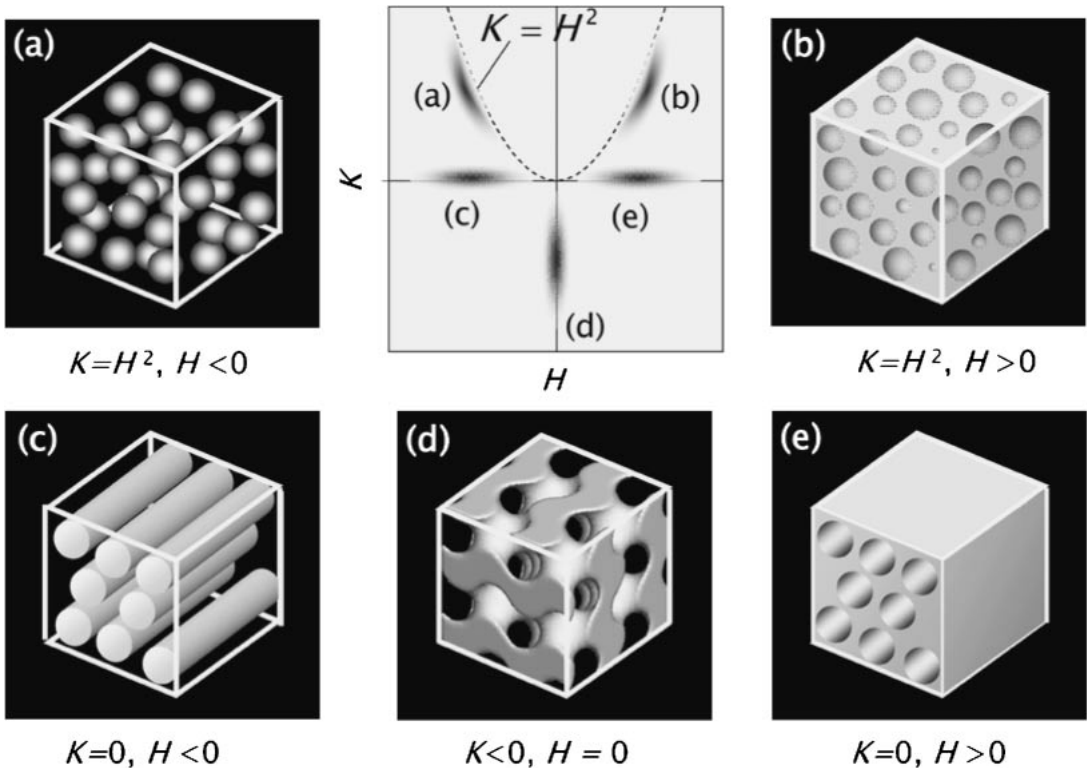

Fig. 13. Probability density distributions of mean and Gaussian curvatures and corresponding typical two-phase structures.

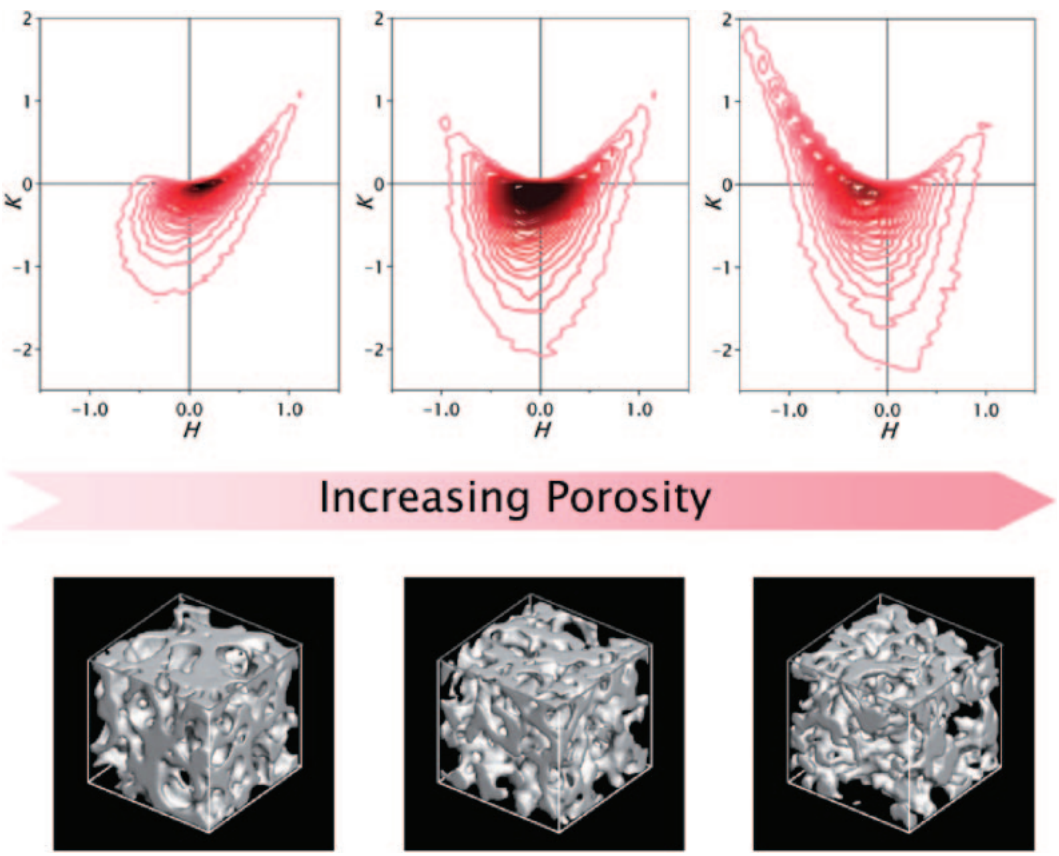

Fig. 14. Measured curvature distributions of macroporous silica gels with comparable pore size and varied porosities.

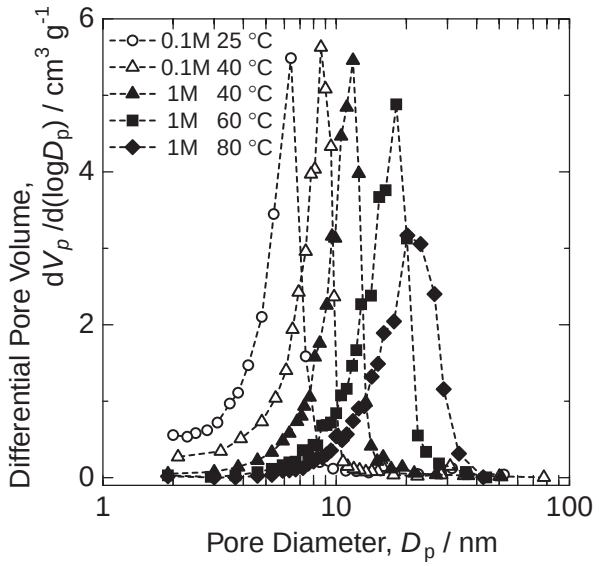

Fig. 15. Differential pore size distribution of gels aged under different conditions (immersion in aqueous ammonia).

ammona in situ. Acid-catalyzed alkoxy-derived silica gels are highly tenuous in the presence of mother liquor (before drying). This is especially true when strongly hydrogen-bonding molecules are present in the hydrolysis–polycondensation system where the aggregation behavior as well as the resultant structure of siloxane oligomers are directly influenced. In the presence of substances with poly(oxyethylene) units, the average connectivity of siloxane oligomers becomes lower, which enhances the dissolution–reprecipitation reactions under basic and/or hydrothermal conditions. The preferential dissolution of gel network sites with small positive curvature and subsequent reprecipitation onto those with small negative curvature results in the reorganization of smaller pores into larger pores (the so called Ostwald ripening mechanism).

Figure 15 shows the differential pore size distribution curves of heat-treated gels after aging in the wet state under various ammonia concentration and/or temperature conditions. Since the equilibrium solubility of amorphous silica increases at higher temperature and under pH conditions typically higher than 10, the median size of resultant mesopores increase at higher ammonia concentration and temperature. Due to the presence of interconnected macropores, the external solution can easily penetrate through the gel specimen (by auxiliary pumping if needed), and the diffusion of the solution into wet gel skeletons of typically a few micrometers becomes a rate-determining step of the solvent exchange processes. The NMR and SAXS (small-angle X-ray scattering) measurements proved that the chemical reorganization of initially microporous network into that with sharply distributed mesopores takes place on the time scale of a few hours.[22] These mesopore formation processes take place within the pre-formed micrometer-sized gel skeletons, so that the size of mesopores can be controlled independently of the macropore size unless the local dissolution of the gel skeletons causes significant deformation of the whole macroporous framework during the solvent exchange.

2.2 Supramolecular Templating of Mesopores. The dissolution–reprecipitation processes of the randomly crosslinked highly hydroxylated silica network results in an amorphous mesoporous network. In addition to the size distribution, further control over the pore shape and connectivity is desired. For the purpose of obtaining mesopores with higher degrees of order in pore size, shape, and spatial arrangement, the supramolecular templating is an attractive alternative to the aging process. It has been found that several kinds of cationic and nonionic surfactants can be used to induce the phase separation concurrently with the sol–gel transition.[23–26] The choice of surfactants suitable also to the supramolecular templating of mesopores can realize materials with crystal-like long-range ordered mesopores homogeneously located in the micrometer-sized well-defined gel skeletons.

The key idea to combine the phase separation–gelation and supramolecular templating–precipitation comes from the fact that both processes include a kind of polymerization-induced phase separation. It has been established that cooperative assembly between surfactant micelles and oligomeric oxides enhances the ordered arrangement of the micelles. Highly ordered mesostructure are organized by such cooperative assembly mechanism in generally amorphous oxide networks. Due to relatively strong attractive interactions between micelles and oxides, submicron- to micron-sized particles are precipitated out of the solution in dilute systems under a closed condition. Alternatively, these well-ordered assemblages can be transferred from a solution onto a substrate, accompanied by preferential evaporation of alcoholic solvent. The structure-forming principle is more generally called evaporation-induced self-assembly, EISA.[27] While the physical concentration of the solutes serves to freeze the structure, the preferential loss of alcohol contributes to the formation of highly aligned mesophases. It, therefore, becomes important for the system to be able to freeze the phase-separating (or precipitating) structure by rapid enough sol–gel transition while the continuous feature of dynamically coarsening phase domains is maintained. The timescale of EISA processes is typically on the order of seconds. The phase separation to develop co-continuous domains in a typical silica sol–gel system is also in the range of seconds to minutes.[28] Then, the preferred sequence of the formation of hierarchical macro-mesoporous structure should be: (1) Self-assembly of surfactants and siloxane oligomers proceeds first, and the initial stage of phase separation (or precipitation) starts slightly earlier than the sol–gel transition of the system; (2) before the complete growth of oligomers ready to precipitate, the whole reaction solution reaches the sol–gel transition, where the local mobility is drastically reduced to inhibit the precipitation of discrete precipitates; (3) due to the remaining driving force of phase separation within the gelling network, phase domains develop to form heterogeneities in the length scale of micrometers; (4) local phase domains including surfactant-oligomer self-assemblies are deformed and/or fragmented in the coarsening stages of phase separation; (5) the transient phase-separating structures are finally frozen in the well-crosslinked gel network (Table 2).

Starting from a composition favorable for the formation of co-continuous macroporous structure containing a triblock copolymer Pluronic P123 (EO_{20}-PO_{70}-EO_{20}, EO: ethylene oxide,

Table 2. Starting Composition and Resultant Morphology of the Gel Samples in TMOS–P123–1.0 M HNO_3aq–TMB System (Unit: g)

Sample	TMOS	P123	TMB	1.0 M HNO_3aq	Morphology
MP4	5.15	4.0	—	12.0	Co-continuous
MP4-T045	5.15	4.0	0.45	12.0	Isolated pores
MP4-T065	5.15	4.0	0.65	12.0	Co-continuous
MP4-T085	5.15	4.0	0.85	12.0	Co-continuous
MP4-T090	5.15	4.0	0.90	12.0	Co-continuous
MP4-T125	5.15	4.0	1.25	12.0	Co-continuous
MP4-T310	5.15	4.0	3.10	12.0	Co-continuous

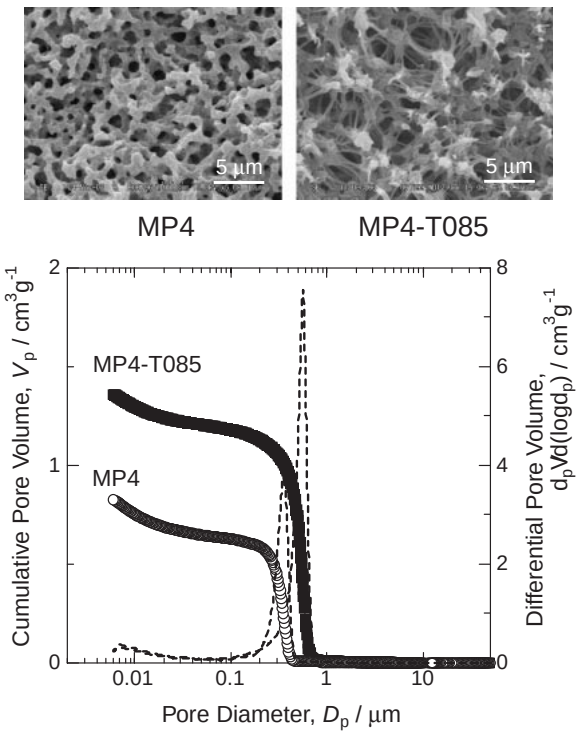

Fig. 16. SEM photographs and mercury porosimetry for MP4 and MP4-T085. Open circle: MP4, Closed square: MP4-T085.

PO: propylene oxide), an additive, 1,3,5-trimethylbenzene (TMB), known to preferentially distributed to the hydrophobic cores of micelles, was introduced to enhance long-range ordering of mesophases.[29] All the characterizations were carried out for the samples dried and heat-treated at 650 °C for 5 h. Figure 16 compares macroporous morphology and pore size distribution of macro-mesoporous monolithic silica gels prepared from the compositions with and without TMB. With an addition of an appropriate amount of TMB relative to that of P123, the shape and long-range order of mesopores are drastically modified. The difference in nitrogen adsorption–desorption isotherms of the two samples, shown in Fig. 17, clearly indicates the formation of cylindrical pores with narrow size distribution accompanied by an increase in pore volume. The long-range ordering of cylindrical pores in 2-dimensional hexagonal symmetry has been confirmed by the XRD results that indicate highly enhanced first peaks with additional higher order peaks.[29] Further, the real-space observations have been performed by FE-SEM and TEM (Fig. 18). Further additions of TMB, however, resulted in the loss of long-range ordered cylindrical pores and a spherical isotropic mesopore system called mesostructured cellular foam, MCF, became dominant. It is noteworthy that the shape of gel skeletons is affected by the anisotropy of mesopores contained in the skeletons; that is, those with cylindrical mesopores exhibit fibrous features.

3. Applications and Products

3.1 Monolithic Separation Media for Ultra-Fast HPLC. High-performance liquid chromatography, HPLC, is one of the most popular liquid-phase analysis techniques. It is used extensively in the fields of organic chemistry, polymer chemistry, biochemistry, and environmental sciences. Columns packed with uniform-size particulate silica gels have been used as separation media for many years and are now technologically well matured. The recent development of sol–gel material synthesis has enabled the manufacture of a revolutionary new type of separation medium, a monolithic column, composed of a single piece of porous silica gel. Important features and advantages of monolithic columns in HPLC fields in comparison with those of conventional particle-packed columns, especially those recognized in recently developing bio-separation fields, are briefly introduced below.

3.1.1 Particle-Packed Columns and Their Limitations: In conventional HPLC technologies, columns packed with oxide particles have been used as standard separation media. Silica gel has been the most popular substance for column packing material. The synthesis, classification, surface modification, dispersion, and packing process of silica gel particles are technologically well established. Over 30 years, the shape of the particles has changed from irregular-shaped to uniform-size spherical form, and the diameter has decreased from several tens microns down to 2–5 microns.[30] The geometrical features of particle-packed columns, nevertheless, have remained unchanged. The overall porosity of the packed column does not exceed 40% by volume, which is the main cause of high liquid-flow resistance (column pressure). The performance of particle-packed columns becomes better with a decrease in the size of particle diameter, while the column pressure is inversely proportional to the particle diameter squared. These factors set a limitation to the improvement of column performance by adopting smaller particles, because the flow rate becomes lower under the limited pumping ability of an ordinary instrumentation.[31] In other words, columns packed with smaller-sized particles separate components better while requiring a higher driving pressure for a constant flow rate of sample solution across the column. Columns packed with 5 micron parti-

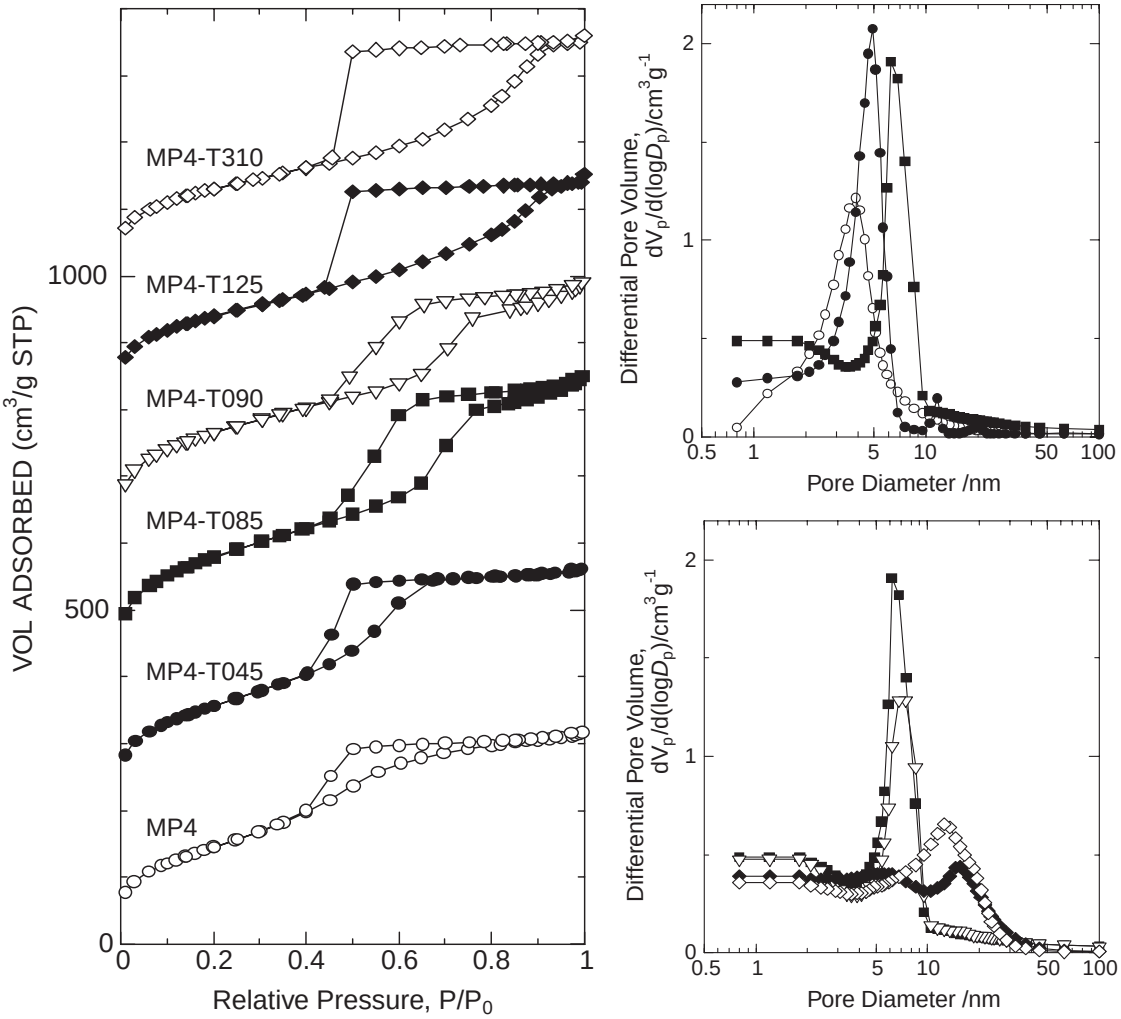

Fig. 17. Nitrogen adsorption–desorption isotherms (Each isotherm is arbitrarily shifted for clarity.) and corresponding pore size distribution curves calculated by BJH method using the adsorption branches of the heat-treated gel samples; Open circle: MP4, Closed circle: MP4-T045, Closed square: MP4-T085, Open downward triangle: MP4-T090, Closed diamond: MP4-T125, Open diamond: MP4-T310.

cles are most widely used as a result of compromise in the above relations between analytical performance and column pressure. This type of column should be used at a relatively low flow rate to obtain best performance.

Column packing technologies are in a matured level, using slurry dispersed with packing particles introduced with the sophisticated pressurizing apparatus into a stainless steel tube. The technologically required column diameter, however, is decreasing for higher sensitivity, reduced solvent consumption and decreased environmental load. Although capillary columns packed with particles are commercially available, the smaller the column diameter, the progressively more difficult it becomes to manufacture capillary columns with high performance and reproducibility.

3.1.2 Monolithic Silica Columns: In the beginning of the 1990's, continuous porous polymer was proposed for a separation medium of HPLC.[32] Almost in parallel, the present author and his colleagues found that, by combining transient domain formation due to phase separation and structure freezing due to sol–gel transition, monolithic macroporous silica with continuous thin gel skeletons and relatively high porosity can be prepared by a liquid-phase processing.[7–9,33,34] The phase separation is induced by the hydrolysis–polycondensation reactions of a silicon alkoxide, leading to the formation of various transitional multi-phase structures including those with co-continuous domains of gel-phase and solvent-phase. By controlling the preparation conditions such as starting composition and reaction temperature, one can induce the sol–gel transition, an irreversible structure-freezing process, concurrently with the above multi-phase structure formation. As a result, monolithic macroporous silica with sharply distributed pore size and skeleton thickness can be manufactured. Compared with polymer-based porous materials represented by poly(styrene-*co*-divinylbenzene), macroporous silica thus prepared exhibit much sharper pore size distribution as well as superior mechanical and thermal stability. The mesopore structure of the monolithic macroporous silica can be controlled by the aging process in the wet stage.[22] The surface chemistry of the resultant mesopores has been found to be similar to that in conventional silica gel particles for packed columns. This means that all the established technologies on surface modification chemistry can be readily transferred to the monolithic silica material.

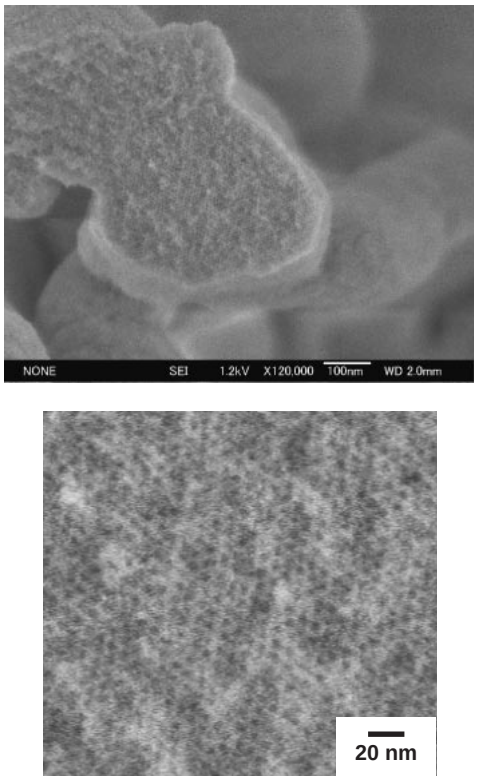

Fig. 18. FE-SEM photographs of heat-treated gel sample with highly ordered 2D-hexagonal mesopores at different magnifications.

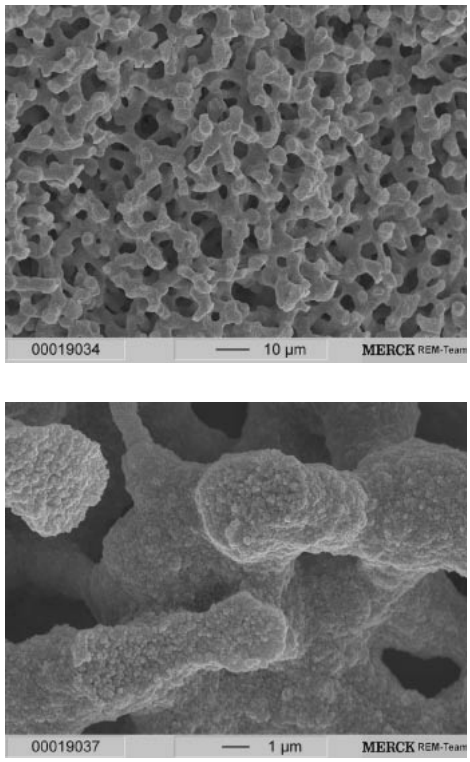

Fig. 19. SEM images of fractured surfaces of monolithic silica gel prepared for HPLC separation medium. Upper image: Co-continuous network of macropores and silica gel skeletons, Lower image: Cross section of silica gel skeleton showing the presence of mesopores (Kindly supplied by Merck KGaA, Darmstadt, Germany).

The separation efficiency of an HPLC column is expressed in the form of a Van Deemter plot which shows the dependence of column plate height, H, column length divided by plate number, on the linear velocity of the mobile phase, u (often termed as H–u curve). In the case of particle-packed columns, H passes through a minimum at relatively low u and then increases almost linearly with u. The highest efficiency, therefore, can only be attained at low mobile phase velocity. Since the increase in H at higher u region stems from the fact that material transfer inside the particle (mainly caused by molecular diffusion) cannot catch up with that in mobile phase flow between the particles, smaller particles gives lower slope and lower H values in the high u region. The limitation arising from the column pressure has inhibited the use of columns packed with smaller particles in an ordinary instrumentation, as described above. The compromise between efficiency and pressure, however, can be avoided in the case of monolithic columns where independently controlled macropore size and gel skeleton thickness can be designed (Figs. 19 and 20).

Typical commercially available Chromolith™ (Chromolith™ is the registered trademark of Merck KGaA, Darmstadt, Germany) columns for analytical chromatography are manufactured by preparing monolithic silica gels with 1.5 micron thick silica skeletons and 2 micron wide macropores into the a shape of column 4.6 mm in diameter and 10–100 mm in length, then encasing them into the "clads" made of fiber-reinforced PEEK (poly(ether–ether–ketone)) resin. They perform better than columns packed with 3.5 micron particles (100000 plates m^{-1}) with less than half the column pressure of 5 micron

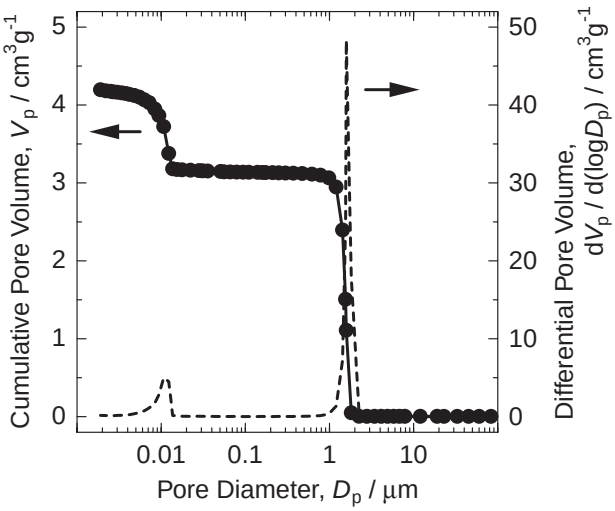

Fig. 20. Hierarchical pore size distribution of monolithic silica gel prepared for HPLC separation medium.

particle-packed columns.[35,36] Figure 21 compares the H–u curves for hexylbenzene analyzed in the reversed phase mode with ODS-modified high-performance 5 micron particles (column length: 150 mm) and ODS-modified monolithic column with 1.5 micron-thick skeletons and 2 micron wide macropores (column length: 30 mm). In spite of considerably shorter column length, the monolithic column performs better in all

the mobile phase velocity regions than the particle-packed column.

With the same column length, monolithic columns give 2–3 times higher mobile phase velocity than particle-packed columns when driven under a given pressure. Due to the weak dependence of column performance on the mobile phase velocity (represented by a gentle slope of H–u curve), monolithic columns can perform separations in 2–3 times shorter times without sacrificing the separation performance at accelerated mobile phase velocities. The connection of several columns, on the other hand, allows the construction of a very high-performance column driven by a pressure comparable to that of an ordinary particle-packed column.

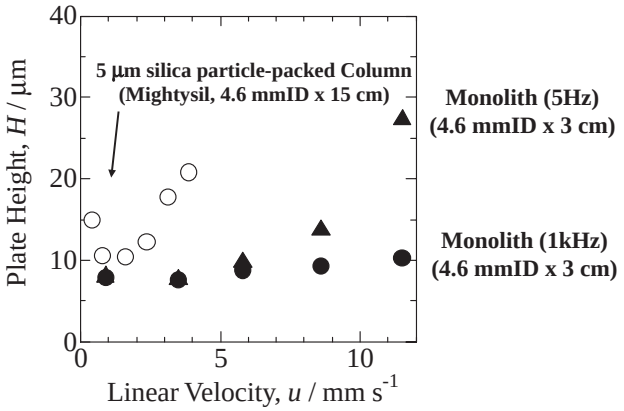

Fig. 21. Van Deemter curves for hexylbenzene determined with an ODS-modified particle-packed column and a monolithic column. Open circle: column packed with ODS-modified 5 micron particles 4.6 mm ID × 150 mm in length; Closed triangle: ODS-modified monolithic column (4.6 mm ID × 30 mm in length) analyzed by normal detecting condition (detection frequency: 5 Hz), Closed circle: ODS-modified monolithic column analyzed by accelerated detecting condition (1 kHz).

Separations of compounds significantly differing in polarity are performed in a so-called solvent gradient mode where the mixing ratio of the mobile phases is changed continuously or stepwise with the elution time. The change in solvent polarity accelerates the elution of substances strongly retained in the stationary phase, making the total analysis time significantly shorter than the case of isocratic elution. The repetition of the solvent gradient elution, however, requires some time to re-equilibrate the column back to the starting mobile phase composition. Monolithic columns which exhibit a low column pressure accelerate repeated separations in the solvent gradient mode not only by reducing the analysis time but also by drastically reducing the re-equilibration time. Moreover, their weak H–u dependence allows one to accelerate the elution of strongly-retained substances by simply increasing the mobile phase velocity while maintaining the separation efficiency. This procedure is called a "pressure gradient" mode, which can be easily performed by programming the pumping system. No re-equilibration time lag is required between repeated operations.[37] A combination of the solvent- and pressure-gradient modes is also available and has been proven to be effective to reduce the total separation time by an order of magnitude (Fig. 22).

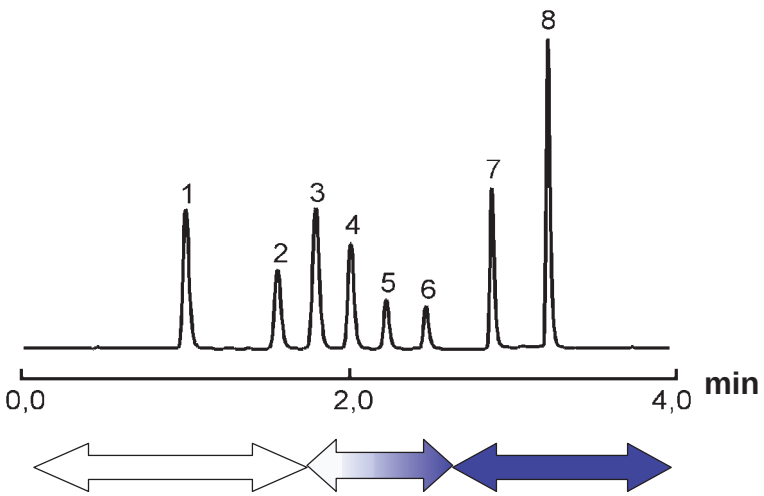

Time min	H_3PO_4 %	Acetonitrile %	Flow rate mL min^{-1}
0.0	65	35	**3**
1.8	54	46	**3**
2.5	20	80	**5**
4.0	20	80	**5**

Samples:
1. **phenol**
2. **2-chlorophenol**
3. **2-nitrophenol**
4. **2,4-dinitrophenol**
5. **4-chloro-3-methylphenol**
6. **6-methyl-2,4-dinitrophenol**
7. **2,4,6-trichlorophenol**
8. **pentachlorophenol**

Column: 4.6mm ID x 10 cm

Fig. 22. Example of combination of solvent- and flow-gradient modes in the separation of mixture of substituted phenols.

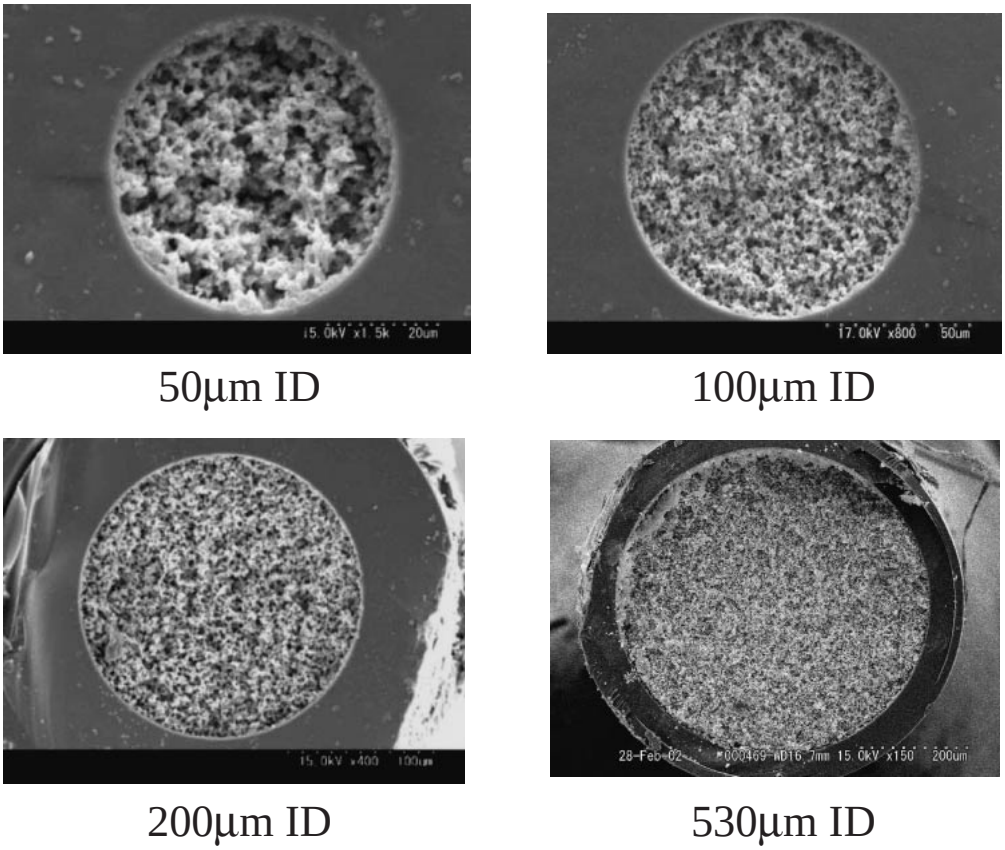

Fig. 23. SEM images of monolithic macroporous silica and methyl-modified siloxane gels prepared in capillaries with various inner diameters.

3.1.3 Challenges to Super-High Performance and Miniaturization: The high porosity and resultant low flow resistance of monolithic columns allow another variation of high-performance column with even smaller macropores and thinner skeletons which can be driven by ordinary pressure to give acceptable mobile phase velocity. This type of monolithic column can exhibit super-high performance comparable to that of a column packed with very small (<1 micron) particles of which the usage has been so far restricted to specialized high-pressure instrumentation or at very low mobile phase velocity with a limited column length.

For the purpose of fully utilizing the ultra-high performance, the instrumentation should be optimized as well. Technical challenges are seen especially in high-pressure pumping and quick-response detection systems. For example, the super-high speed separations can be confirmed only by enhancing the time resolution of the detection at increased sampling frequency (Fig. 21).

Smaller diameter columns are known to exhibit higher sensitivity and reduced consumption of mobile phase solvent and sample substances. In the case of particle-packed columns, with the decrease of diameter of tubes or capillaries, it becomes progressively more difficult to pack them with particles uniformly and reproducibly in view of chromatographic separations. Monolithic columns with PEEK clad also suffer from difficulty in manufacturing when thinner gel pieces should be handled without fracture. The advantage of sol–gel processing, i.e. liquid-phase synthesis, here manifests itself to overcome these obstacles. Compared with the packing of particles, the filling of a reaction solution into small spaces such as capillaries and micro-fabricated channels is much easier. The problematic shrinkage and deformation, which are inherent in sol–gel processing, can be better avoided as at least one of the dimensions of the gel becomes smaller. Figure 23 shows the SEM images of fractured sections of monolithic columns prepared inside the fused silica capillaries with varied inner diameters.[38] Capillary columns have advantages in that they require no cladding process, and can be easily prepared in desired length. The chromatographic instrumentation for capillary columns, again, is still on its way to optimization, especially with thinner columns. High precision micro-pumps and mixers for stabilized mobile phase velocity and constant solvent gradient as well as highly sensitive on-column detectors are necessary to make the best use of monolithic capillary columns.

3.1.4 Applications in Bio-Separation Fields: Since HPLC is a separation method based on the chemical interaction between a solute molecule and the surface of stationary phase, the importance of HPLC analysis is rapidly increasing in so-called "proteomics" and "metabolomics," analysis of a series of proteins or metabolites in various stages of biological activities in living cells, where the chemical interaction in a liquid phase plays an important role. In proteome analysis, the number of proteins to be separated and identified is estimated to reach millions with a diverse range of abundances. Higher sensitivity as well as higher throughput of the analytical method is therefore mandatory.

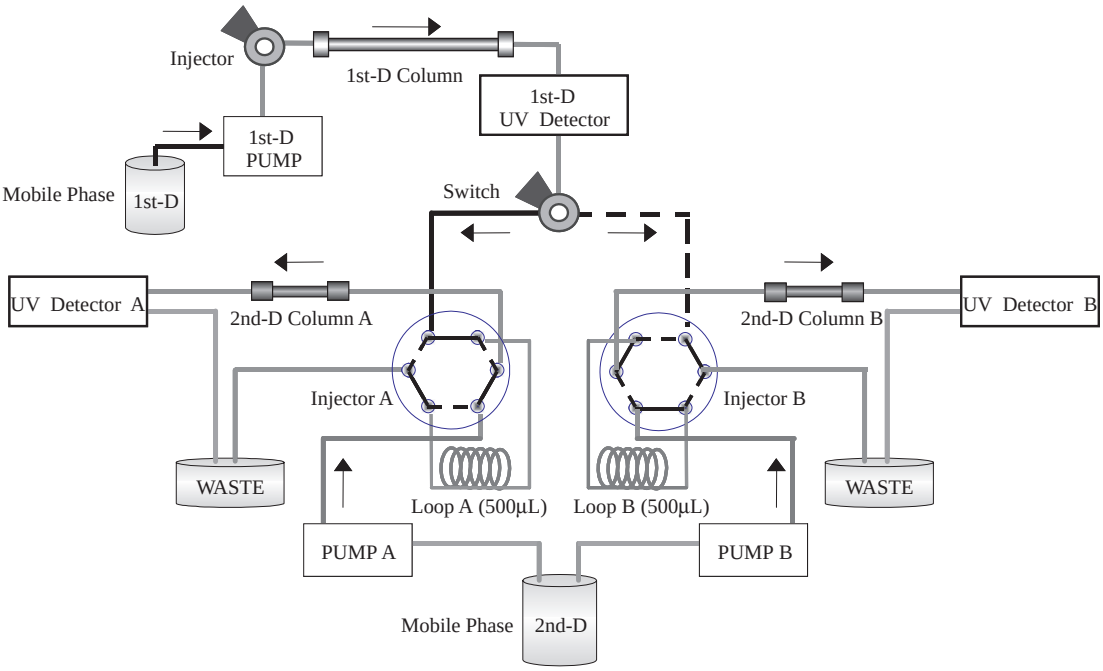

Fig. 24. Schematic illustration of 2D HPLC system utilizing the monolithic HPLC columns as 2nd dimension separation media. Components separated on the 1st dimension are distributed alternately to the 2nd dimension columns by "Switch" bulb as indicated by solid and dotted lines.

Monolithic silica columns exhibit up to an order higher performance than the conventional columns not only for smaller molecules but also for larger molecules such as polypeptides and even proteins. The miniaturized versions of monolithic columns, including those integrated into microchips with multiple liquid-flow channels, will contribute to improve the performance of LC/MS (Liquid Chromatography coupled with Mass Spectrometry) and revolutionize the proteome analysis methodology. Specifically, in the two-dimensional chromatography (fractions separated on the first dimension column are respectively separated in the second dimension columns), the peak capacity becomes the multiplication of those of the first- and second-dimension columns. Thus, it will be possible for this method to compete with the well-established two-dimensional poly(acrylamide) gel electrophoresis, 2D-PAGE, for a wide range of bio-related molecules. Figure 24 schematically illustrates a two-dimensional HPLC instrument where the components separated on the "1st-D column" are alternately distributed either to "2nd-D column A" or "2nd-D column B" every 30 seconds using a switching bulb. As each analysis on "2nd-D column A" or "2nd-D column B" is finished within 60 seconds, the repeated analysis until the end of elutions on the first dimension constitutes the 2-dimensional separations.[39,40] Another run with reversed distribution order in the second dimension completes the total set of 2D separations.

HPLC columns which can specifically separate phosphorus-containing compounds can be prepared using either pure titania gels or silica gels with their macropore surfaces modified with thin titania coatings.[41,42] Combined with the fast separation of larger molecules such as proteins with the monolithic silica columns, the titania-modified monolithic columns will greatly accelerate the analysis of a vast number of phosphorus-containing compounds found in proteomics and metabolomics studies.

Lab-on-a-chip technology is based on micro-fabricated flow networks that substitute macro-scale pipelines where various kinds of chemical/physical processes are performed utilizing the advantages of interfacial phenomena in confined spaces. Similarly to the capillary columns, the monolithic porous silica can serve as an efficient separation medium or catalyst/substrate support for chemical reactions. Multi-capillary or micro-fabricated multi-channel columns suitable for high-throughput highly integrated bio-analysis are on their way to development.

3.2 Future Challenges and Additional Applications. Monolithic materials with highly controlled inner surfaces such as well-defined hierarchical pores can be used in many of the areas where the particle-packed structure has been playing an important role. Their low flow resistance (high permeability) and enhanced accessibility to the nano-scaled surfaces in liquid phase are advantageous to every reaction/separation/purification processes.

Liquid-phase catalytic reactions can be enhanced in a device composed of immobilized enzyme or catalyst in general.[43] Kato et al. recently prepared a flow-through bio-reactor made of macroporous silica monolith support incorporated with immobilized trypsin.[44] Chromatography in larger dimensions for preparative and process purposes will also benefit by the use of monolithic columns prepared in appropriate module structures. Similarly, materials for solid-phase extraction, SPE, purposes can be easily designed to exhibit superior permeability and extraction efficiency.[45,46]

The propagation of light in a dielectrically disordered medium is modified by multiple scattering and interference. In strongly scattering media with a large refractive index variation on a length scale comparable to light wavelength, interference of multiply scattered light brings about various interest-

ing phenomena such as photon localization. The controllable well-defined macroporous morphology has an advantage in tuning the scattering intensity of laser light in visible range. Although the macroporous morphology is essentially isotropic (disordered) beyond the nearest neighbor correlation length, the size and volume of pores can be precisely controlled compared with other scatterers such as aggregated particles. The successful preparation of well-defined macroporous titania monoliths enabled one to directly compare the scattering behavior of a comparable structure with different chemical compositions (a-SiO_2 and rutile).[47] Due to the difference in refractive index between a-SiO_2 and rutile, 1.4 and 2.7, respectively, the values of mean free path of the laser light of 488 nm exhibited a large difference in a-SiO_2 and in rutile.

4. Conclusion

Polymerization-induced phase separation in oxide sol–gel systems is unique in that a wide variety of transient multiphase structures are frozen in the gelled samples. Most tri- and tetra-functional siloxane-based gelling systems can be designed to exhibit phase separation parallel to the sol–gel transition. Recent success of inducing concurrent phase separation and sol–gel transition in colloidal dispersion systems implies that the phenomenon is independent of the mechanism of gelation (chemical polymerization or physical aggregation). The very essential requirement is simply "competitive" phase separation and sol–gel transition both in length scale and in time scale.

Recent advances in structural characterization of multiphase systems by LSCM made it possible to quantitatively evaluate the local structures in a non-destructive manner, which can provide complimentary information to that obtained by conventional methods. Time-resolved observation of specific phase-separation pathways will become possible and provide much more information than that obtained by scattering methods.

Macropore control of silica and siloxane gels is now a well-established method to fabricate gel-based devices in various forms. With an extension of the material shape and size, the effect of spatial confinement on the structure development becomes significant. Deeper understanding is still needed to completely control the morphology even in the miniaturized spaces.

Further development of chemical modification of the pore surfaces as well as impregnating functional molecules will enhance the application of the well-defined hierarchically porous material. The successful introduction of supramolecularly templated mesostructures into the well-defined macroporous framework will offer additional possibilities to accommodate molecules, bio-polymers and even living cells complexed with the surfactant mesophases. Continuous efforts are being made to integrate a wide variety of highly-ordered mesophases into well-defined assemblies in longer length scales with extended chemical compositions.

Most of the works presented here have been performed at the Department of Material Chemistry, Graduate School of Engineering, Kyoto University where the author started his career as a researcher. The author thanks all the academic staff members of the Inorganic Structural Chemistry laboratory, represented by Emeritus Prof. Naohiro Soga. Hearty thanks also go to the students who made efforts in many parts of the experiments. Prof. Nobuo Tanaka at Kyoto Institute of Technology, Dr. Hiroyoshi Minakuchi at Kyoto Monotech Corp., and Dr. Gerhard Wieland at Merck KGaA contributed a lot to the development of monolithic silica columns now commercialized worldwide. Prof. Hiroshi Jinnai and Dr. Yukihiro Nishikawa kindly provided invaluable information and practical experimental methods of LSCM observation as well as sophisticated digital data processing.

The support from Japan Science and Technology Agency by PRESTO program "Structural Ordering and Physical Properties" during 2000–2003 period is especially acknowledged. The present work was partly supported by a Grant-in-Aid for Scientific Research (No. 15206072) from the Ministry of Education, Culture, Sports, Science and Technology, Japan.

References

1 M. E. Nordberg, *J. Am. Ceram. Soc.* **1944**, *27*, 299.
2 C. J. Brinker, G. W. Scherer, *Sol-Gel Science: The Physics and Chemistry of Sol-Gel Processing*, Academic Press, New York, **1990**.
3 P. J. Flory, *Principles of Polymer Chemistry*, Cornell University Press, Ithaca, New York, **1971**.
4 P. G. De Gennes, *Scaling Concepts in Polymer Physics*, Cornell University Press, Ithaca, New York, **1979**.
5 H. Kaji, K. Nakanishi, N. Soga, *J. Sol-Gel Sci. Technol.* **1993**, *1*, 35.
6 K. Nakanishi, T. Yamato, K. Hirao, *Mater. Res. Soc. Symp. Proc.* **2002**, *726*, Q9.7.1.
7 K. Nakanishi, N. Soga, *J. Am. Ceram. Soc.* **1991**, *74*, 2518.
8 K. Nakanishi, N. Soga, *J. Non-Cryst. Solids* **1992**, *139*, 1.
9 K. Nakanishi, H. Komura, R. Takahashi, N. Soga, *Bull. Chem. Soc. Jpn.* **1994**, *67*, 1327.
10 T. Hashimoto, M. Itakura, H. Hasegawa, *J. Chem. Phys.* **1986**, *85*, 6118.
11 K. Kanamori, N. Ishizuka, K. Nakanishi, K. Hirao, H. Jinnai, *J. Sol-Gel Sci. Technol.* **2003**, *26*, 157.
12 K. Kanamori, K. Nakanishi, K. Hirao, H. Jinnai, *Langmuir* **2003**, *19*, 5581.
13 R. D. Shoup, in *Colloid and Interface Science*, ed. by M. Kerker, Academic Press, New York, **1976**, Vol. 3, p. 63.
14 J. Konishi, K. Fujita, K. Nakanishi, K. Hirao, *Mater. Res. Soc. Symp. Proc.* **2004**, *788*, L8.14.1.
15 H. Nishino, R. Takahashi, S. Sato, T. Sodesawa, *J. Non-Cryst. Solids* **2004**, *333*, 284.
16 Y. Tomita, R. Takahashi, S. Sato, T. Sodesawa, M. Otsuda, *J. Ceram. Soc. Jpn.* **2004**, *112*, 491.
17 R. Takahashi, S. Sato, T. Sodesawa, T. Azuma, *J. Sol-Gel Sci. Technol.* **2004**, *31*, 373.
18 A. Yachi, R. Takahashi, S. Sato, T. Sodesawa, K. Oguma, K. Matsutani, N. Mikami, *J. Non-Cryst. Solids* **2005**, *351*, 331.
19 H. Jinnai, K. Nakanishi, Y. Nishikawa, J. Yamanaka, T. Hashimoto, *Langmuir* **2001**, *17*, 619.
20 H. Saito, K. Nakanishi, K. Hirao, H. Jinnai, K. Morisato, H. Minakuchi, *Mater. Res. Soc. Symp. Proc.* **2005**, *847*, EE9.2.1.
21 Y. Nishikawa, H. Jinnai, T. Koga, T. Hashimoto, S. T. Hyde, *Langmuir* **1998**, *14*, 1242.
22 K. Nakanishi, R. Takahashi, T. Nagakane, K. Kitayama,

N. Koheiya, H. Shikata, N. Soga, *J. Sol-Gel Sci. Technol.* **2000**, *17*, 191.
23 K. Nakanishi, T. Nagakane, N. Soga, *J. Porous Mater.* **1998**, *5*, 103.
24 Y. Sato, K. Nakanishi, K. Hirao, H. Jinnai, M. Shibayama, Y. B. Melnichenko, G. D. Wignall, *Colloids Surf., A* **2001**, *187/188*, 117.
25 K. Nakanishi, Y. Sato, Y. Ruyat, K. Hirao, *J. Sol-Gel Sci. Technol.* **2003**, *26*, 567.
26 K. Nakanishi, *Mater. Res. Soc. Symp. Proc.* **2004**, *788*, L7.5.1.
27 C. J. Brinker, Y. Lu, A. Sellinger, H. Fan, *Adv. Mater.* **1999**, *11*, 579.
28 H. Kaji, K. Nakanishi, N. Soga, T. Inoue, N. Nemoto, *J. Sol-Gel Sci. Technol.* **1994**, *3*, 169.
29 T. Amatani, K. Nakanishi, K. Hirao, T. Kodaira, *Chem. Mater.* **2005**, *17*, 2114.
30 R. P. W. Scott, *Silica Gel and Bonded Phases*, John Wiley & Sons, Chichester, **1993**.
31 H. Poppe, *J. Chromatogr., A* **1997**, *778*, 3.
32 F. Svec, J. M. Frechet, *Anal. Chem.* **1992**, *64*, 820.
33 K. Nakanishi, Y. Sagawa, N. Soga, *J. Non-Cryst. Solids* **1991**, *134*, 39.
34 K. Nakanishi, *J. Porous Mater.* **1997**, *4*, 67.
35 H. Minakuchi, K. Nakanishi, N. Soga, N. Ishizuka, N. Tanaka, *Anal. Chem.* **1996**, *68*, 3498.
36 N. Tanaka, H. Kobayashi, K. Nakanishi, H. Minakuchi, N. Ishizuka, *Anal. Chem.* **2001**, *73*, 420A.
37 K. Cabrera, D. Lubda, H.-M. Eggenweiler, H. Minakuchi, K. Nakanishi, *J. High Resolut. Chromatogr.* **2003**, *23*, 93.
38 N. Ishizuka, H. Minakuchi, K. Nakanishi, N. Soga, H. Nagayama, K. Hosoya, N. Tanaka, *Anal. Chem.* **2000**, *72*, 1275.
39 N. Tanaka, H. Kimura, D. Tokuda, K. Hosoya, T. Ikegami, N. Ishizuka, H. Minakuchi, K. Nakanishi, Y. Shintani, M. Furuno, K. Cabrera, *Anal. Chem.* **2004**, *76*, 1273.
40 H. Kimura, T. Tanigawa, H. Morisaka, T. Ikegami, K. Hosoya, N. Ishizuka, H. Minakuchi, K. Nakanishi, M. Ueda, K. Cabrera, N. Tanaka, *J. Sep. Sci.* **2004**, *27*, 897.
41 Y. Kimura, S. Shibasaki, K. Morisato, N. Ishizuka, H. Minakuchi, K. Nakanishi, M. Matsuo, T. Amachi, M. Ueda, K. Ueda, *Anal. Biochem.* **2004**, *326*, 262.
42 S. Miyazaki, M. Y. Miah, K. Morisato, Y. Shintani, T. Kuroha, K. Nakanishi, *J. Sep. Sci.* **2005**, *28*, 39.
43 R. Takahashi, S. Sato, T. Sodesawa, K. Arai, M. Yabuki, *J. Catal.* **2005**, *229*, 24.
44 M. Kato, K. Inuzuka, K. Sakai-Kato, T. Toyo'oka, *Anal. Chem.* **2005**, *77*, 1813.
45 Y. Shintani, X. Zhou, M. Furuno, H. Minakuchi, K. Nakanishi, *J. Chromatogr., A* **2003**, *985*, 351.
46 S. Miyazaki, K. Morisato, N. Ishizuka, H. Minakuchi, Y. Shintani, M. Furuno, K. Nakanishi, *J. Chromatogr., A* **2004**, *1043*, 19.
47 K. Fujita, J. Konishi, K. Nakanishi, K. Hirao, *Appl. Phys. Lett.* **2004**, *85*, 5595.
48 J. Konishi, K. Fujita, K. Nakanishi, K. Hirao, *Chem. Mater.* **2006**, *18*, 864.

Kazuki Nakanishi was Research Associate (1986–1995), and Associate Professor (1995–2005) at the Department of Material Chemistry, Graduate School of Engineering, Kyoto University. He is now Associate Professor of Department of Chemistry, Graduate School of Science, Kyoto University. He received a Doctor of Engineering Degree from Kyoto University in 1991. He was also a research member of "Structural Ordering and Physical Properties," PRESTO, Japan Science and Technology Agency during 2000–2003. He received *D.R. Ulrich Award* at the "9th International Workshop on Glasses, Ceramics, Hybrids, and Nanocomposites from Gels" in 1997 and the *ICG Award in memorium of Prof. Vittorio Gottardi* from the International Committee on Glass in 1999 for his outstanding works on sol–gel and glass science and technology. He became interested in the competitive processes between phase separation and sol–gel transition in 1986 when he started his career as a researcher and is still digging into its depth after 20 years. His research focuses on the integrated design of hierarchically porous materials in ceramics, organic–inorganic hybrids, and colloidal systems.